

Supporting Information

Improved performance of perovskite solar cells by fine-tuning dibenzofuran-based hole transporting materials

*Xuepeng Liu^a, Xianfu Zhang^a, Mingyuan Han^a, Jianlin Chen^a, Ghadari Rahim^b,
Yongpeng Liang^a, Botong Li^a, Songyuan Dai^{a*}*

^aBeijing Key Laboratory of Novel Thin-Film Solar Cells, School of New Energy, North China Electric Power University, Beijing 102206, China

^bComputational Chemistry Laboratory, Department of Organic and Biochemistry, Faculty of Chemistry, University of Tabriz, Tabriz, 5166616471, Iran.

E-mail: sydai@ncepu.edu.cn

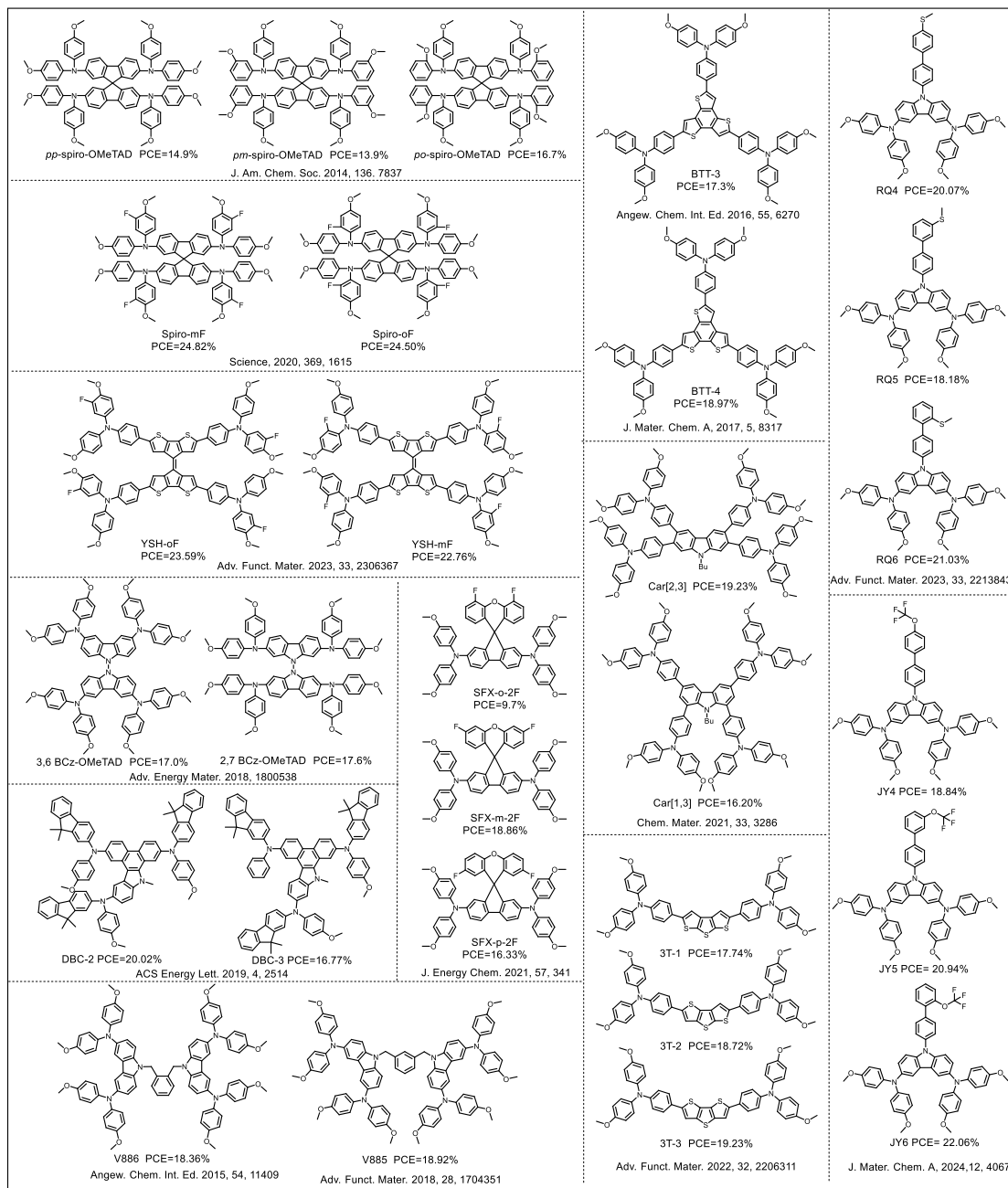


Fig. S1 Brief summary of the reported isomeric HTMs and the device efficiency in PSCs.

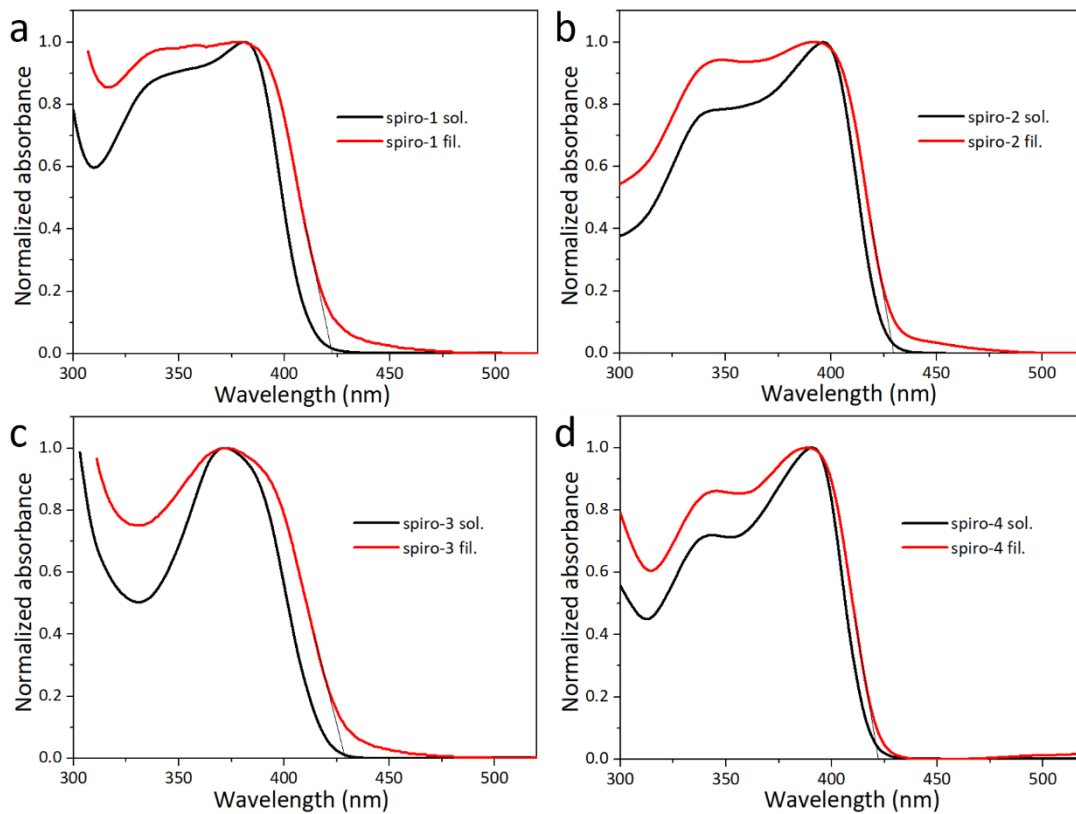


Fig. S2 UV-vis absorption spectra of spiro-2, spiro-3, spiro-4 and spiro-1 in dilute dichloromethane solution and thin film state.

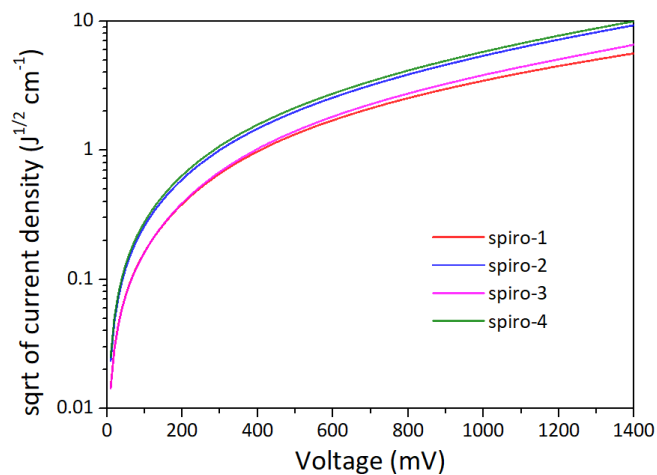


Fig. S3 SCLC J - V characteristics of different HTM-based hole-only devices

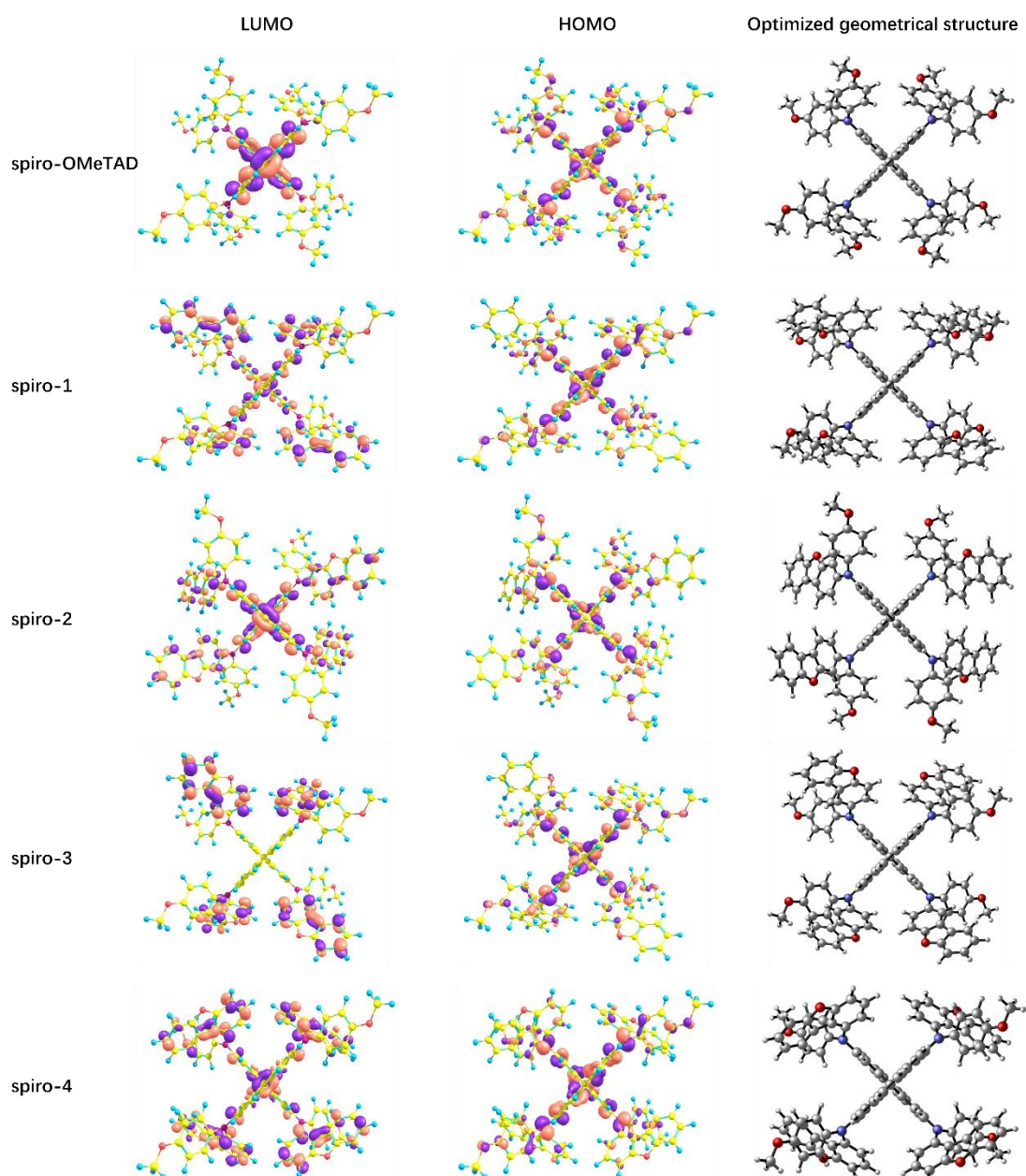
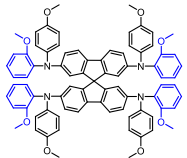
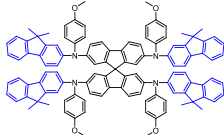
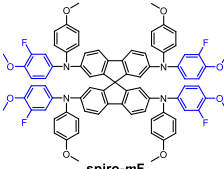
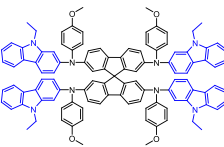
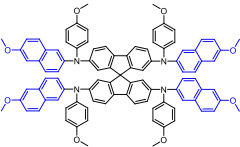
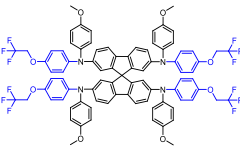
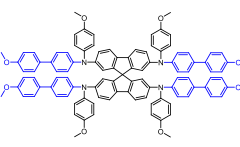
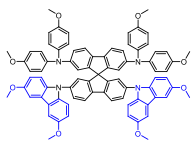
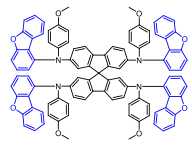


Fig. S4 Frontier molecular orbital distributions and optimized geometrical structures, of the investigated molecules.

Table S1 Summary of molecular properties and device performance for the reported similar reported molecules compared with our studied HTMs. The blue bond on the structure illustrate the structural difference with spiro-OMeTAD.

designatio n	Molecular structure	HOMO level (eV) and PCE of the	HOMO level and PCE of spiro- OMeTAD	Reduction value of HOMO compared with	T _g (°C)	Reference

		studied HTM	in the work	spiro- OMeTAD		
po-spiro- OMeTAD		-5.31 eV 16.7%	-5.22 eV 15.2%	0.09 eV	-	J. Am. Chem. Soc., 2014, 136, 7837
DM		-5.27 eV 23.2%	-5.22 eV 21.3%	0.05 eV	161	Nat. Energy, 2018, 3, 682
Spiro-mF		-5.19 eV 24.82%	-4.97 eV 23.44%	0.22 eV	120 ^a	Science, 2020, 369, 1615
SC		-5.26 eV 21.78%	-5.22 eV 20.73%	0.04 eV	164	Chem. Mater., 2021, 33, 285
spiro- Naph		-5.05 eV 24.43%	-5.01 eV 23.95%	0.04 eV	147	Nat. Photon., 2022, 16, 119
Spiro- 4TFEAD		-5.25 eV 21.11%	-5.15 eV 20.44%	0.10 eV	140	Solar RRL, 2022, 6, 2100944
DP		-5.18 eV 25.24%	-5.10 eV 24.34%	0.09 eV	149	Angew. Chem. Int. Ed. 2023, 62, e202304350
SF-MPA- MCz		-5.26 eV 24.53%	-5.13 eV 22.95%	0.13 eV	154	Research, 2024, 7, 0332
spiro-4		-5.29 eV 23.38%	-5.10 eV 22.10%	0.19 eV	163	This work

^a T_g value of Spiro-mF is measured by ourself (which is not reported in published work, Science, 2020, 369, 1615), as illustrated in Fig. S5, and Spiro-mF is synthesized in our lab.

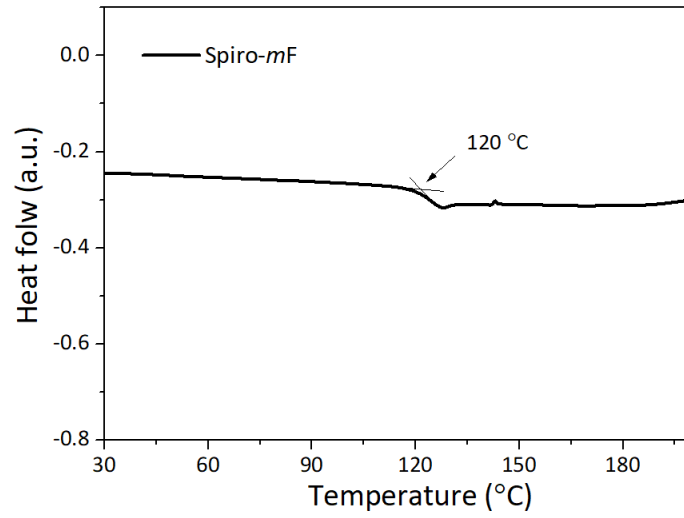


Fig. S5 DSC measurement of Spiro-*m*F.

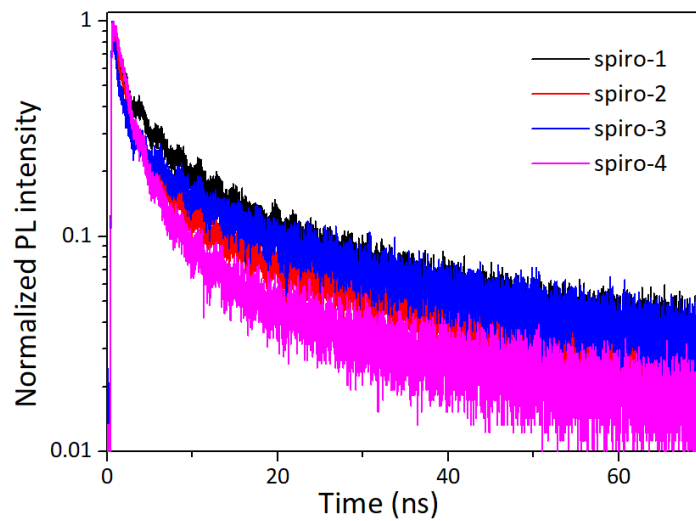


Fig. S6 Time-resolved photoluminescence spectra of pristine perovskite films, or coated with various HTMs

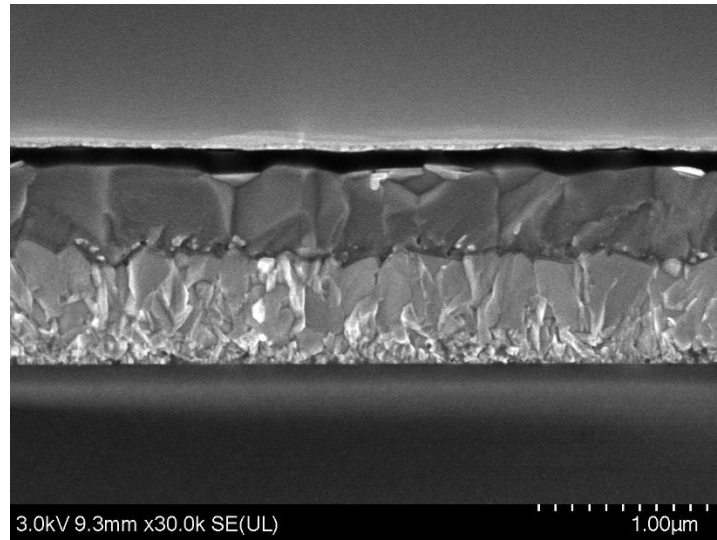


Fig. S7 Cross-sectional scanning electron microscopy of a representative device.

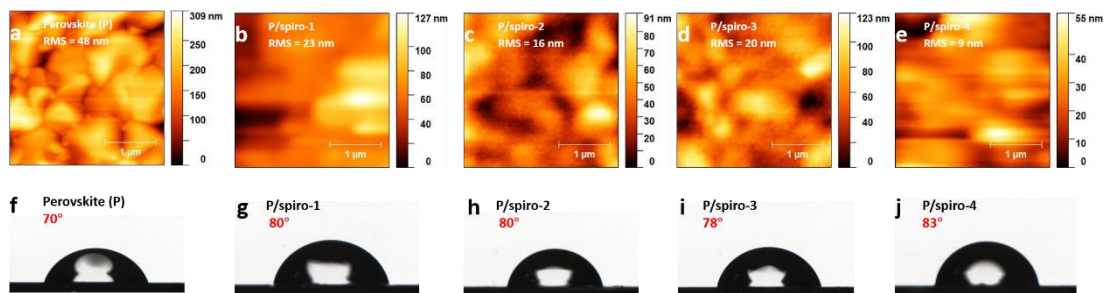


Fig. S8 (a-e) AFM images and (f-j) contact-angle measurements of the perovskite layer or perovskite deposited with different HTMs.

Table S2 Mean values with standard deviation (STDEV) of photovoltaic parameters (reverse scan direction) of PSCs with different HTMs, the average values were derived from 16 devices.

HTM	V_{oc} (V)	J_{sc} (mA cm^{-2})	FF (%)	PCE (%)
spiro-1	1.10±0.02	24.76±0.05	69.69±1.20	19.04±0.47
spiro-2	1.14±0.01	24.65±0.07	77.44±1.36	21.69±0.51
spiro-3	1.11±0.02	24.83±0.07	74.13±0.81	20.36±0.45
spiro-4	1.15±0.01	24.92±0.05	78.25±1.34	22.49±0.51
spiro-OMeTAD	1.14±0.01	24.93±0.06	76.25±0.93	21.71±0.29

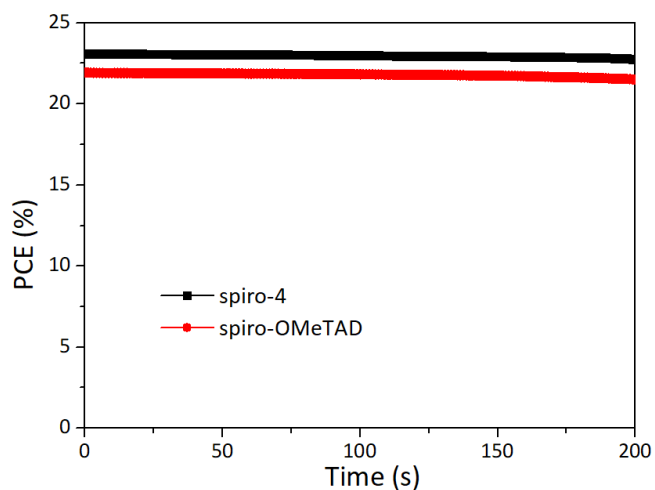


Fig. S9 Steady-state maximum power output of the device employing spiro-4 or spiro-OMeTAD.

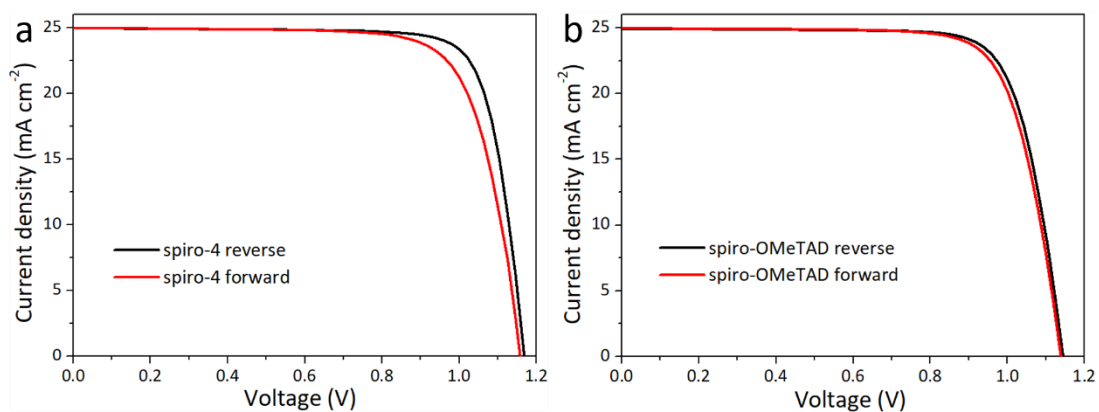


Fig. S10 *J-V* curves of the devices with spiro-OMeTAD or spiro-4 as HTMs measured from reverse and forward scans.

Table S3 Photovoltaic parameters of best PSCs with spiro-4 or spiro-OMeTAD and obtained through reverse and forward scans for Fig. S5.

HTM	Scan direction	V_{oc} (V)	J_{sc} (mA cm^{-2})	FF (%)	PCE (%)
spiro-4	reverse	1.17	24.98	80	23.38
	forward	1.16	24.96	76	21.84
spiro-OMeTAD	reverse	1.15	24.95	77	22.10
	forward	1.14	24.97	76	21.65

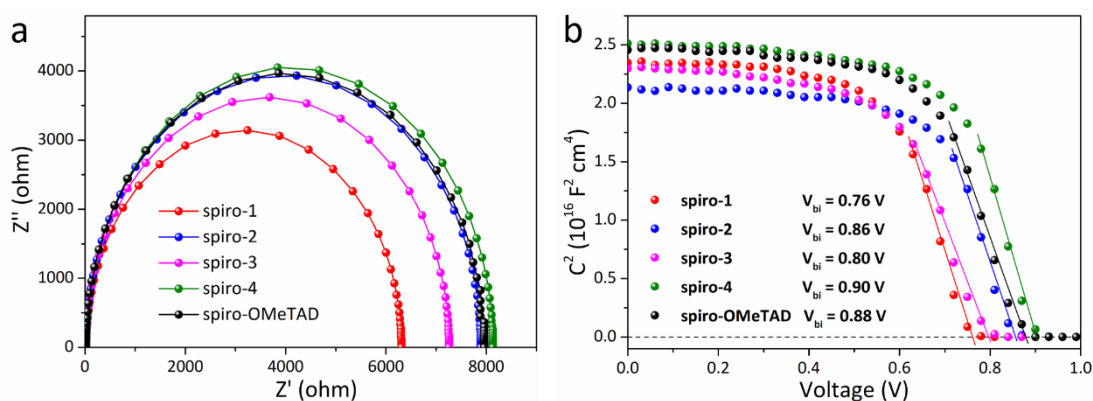


Fig. S11 (a) Nyquist plots of the EIS test, (b) Mott–Schottky plots of the prepared PSCs with different HTMs.

Device fabrication

The device fabrication process is mainly done refer to our previous reports.^{1,2} In detail, FTO glass plates were sequentially cleaned in soapy water, deionized water and ethanol for 15 min with sonication. Using spray pyrolysis techniques, a precursor solution of 0.7 mL titanium diisopropoxide bis(acetylacetonate) mixed in 14 mL isopropanol was used to deposit the compact TiO_2 layer at 500°C on a clean FTO substrate. Mesoporous TiO_2 layer was created by spin-coating a diluted particle TiO_2 paste (Dyesol 30NR-T, 1:12 w/w diluted in ethanol) at 3000 rpm for 30s on the previously mentioned substrate. The substrates were then annealed for 30 minutes at a temperature of around 500°C . The $\text{Cs}_{0.05}\text{FA}_{0.95}\text{PbI}_3$ perovskite precursor solution includes PbI_2 (1.53 M), FAI (1.33 M), CsI (0.09 M) and MAI (0.4 M), dissolved in a mixed solvent of DMF and DMSO solution (1000 μL , volume ratio 8:2). The spin-coating process was carried out at 1000 rpm for 10 seconds, and then at 5000 rpm for 30 seconds. During the last 10 seconds of the process, 110 μL of chlorobenzene (CB) is drip-coated onto the rotating substrate. The obtained substrate was immediately heated at 100°C for 30 min and 150°C for 10 min on the hotplate. The HTM was then coated on the substrate by spin-coating at 5000 rpm for 30 s. For the dibenzofuran-terminated HTMs, the concentration is 50 mg mL^{-1} after preliminary optimization, respectively, which is doped with 20 μL of 4-tert-butylpyridine and 11 μL of lithium bis(trifluoromethylsulfonyl)imide (520 mg mL^{-1} in acetonitrile) and 6 μL tris (2-(1H-pyrazol-1-yl)-4-tert-butyl-pyridine)-cobalt(III) tris (bis (trifluoromethylsulfonyl) imide) (300 mg mL^{-1} in acetonitrile). spiro-OMeTAD (99.8%, HPLC, Xi'an Polymer Light Technology Corp.) were dissolved in chlorobenzene (73.5 mg mL^{-1}) with 29 μL of 4-tert-butylpyridine and 17 μL of lithium bis(trifluoromethylsulfonyl)imide (520 mg mL^{-1} in acetonitrile) and 8 μL tris (2-(1H-pyrazol-1-yl)-4-tert-butyl-pyridine)-cobalt(III) tris (bis (trifluoromethylsulfonyl) imide) (300 mg mL^{-1} in acetonitrile). Finally, a $\sim 70 \text{ nm}$ thick Au counter electrode was deposited on top of above film by thermal evaporation. The active area of the device was defined by a black mask with a size of 0.1225 cm^2 for all measurements.

Characterization

NMR spectra were obtained using a Brücker spectrometer (500 MHz) with chemical shifts against tetramethylsilane (TMS). A UV-vis spectrophotometer (UV-3600 plus, Shimadzu Co. Ltd., Japan) is used to measure the ultraviolet-visible (UV-vis) spectra of the compounds under investigation. On the fluorescence spectrophotometer, the PL measurements of HTMs were captured (Hitachi F-4600, Japan). The decomposition temperature of the developed materials was measured with a heating rate of $15^{\circ}\text{C min}^{-1}$ under nitrogen atmosphere (TGA, PerkinElmer, STA-8000). With a scan rate of $15^{\circ}\text{C min}^{-1}$, differential scanning calorimetry (DSC) is performed (METTLER-Toledo DSC1). Using a fluorescence spectrometer (FLS980, Edinburgh, UK) with an excitation wavelength of 488 nm, the PL spectrum of perovskite/HTM films was measured. A 3A grade solar simulator (Newport, USA) with an intensity of 100 mW cm^{-2} and a Keithley 2400 source meter under AM 1.5G were used to test the J-V characteristics. In addition, repeatedly test JV characteristic of high efficiency device in an independent laboratory (National-Local Joint Engineering Laboratory of New Energy Photoelectric Devices, Hebei University, Baoding, China). On the QE/IPCE measurement kit, the incident photon-to-current conversion efficiency (IPCE) was measured (Sofn Instruments Co, LTD, China). The METATEST E3-300 contact angle tester was used to measure the moisture resistance of HTMs.

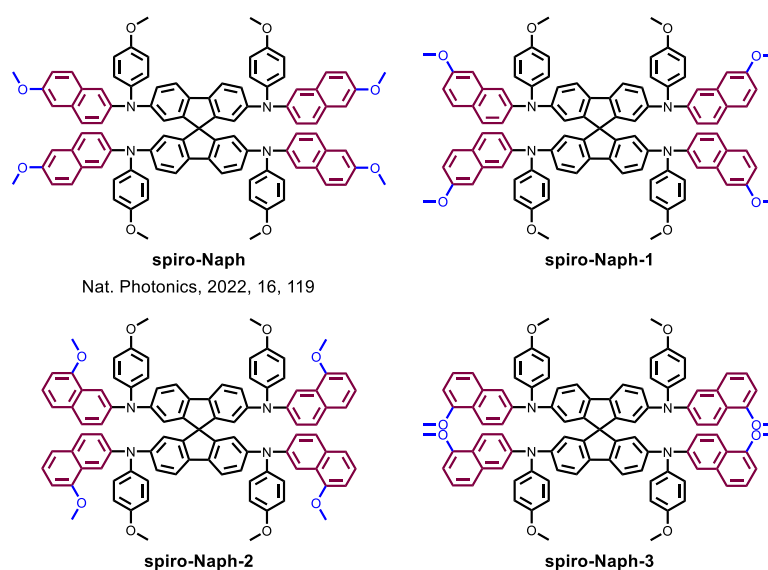


Fig. S12 Molecular structures of spiro-Naph analogues

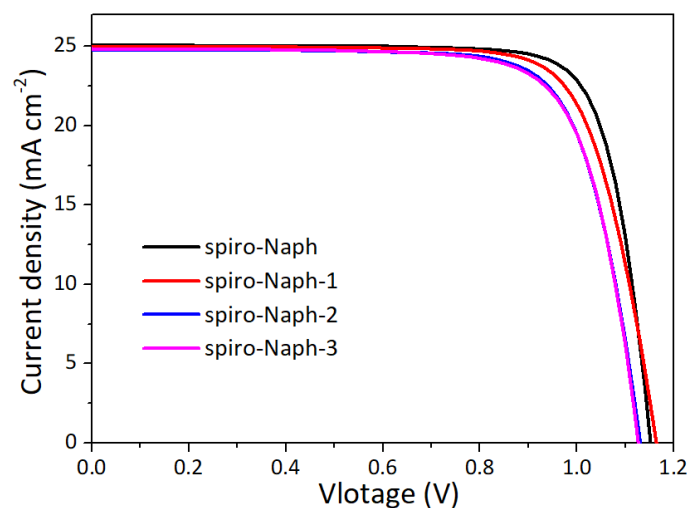


Fig. S13 J – V curves of the best-performing PSCs with spiro-Naph, spiro-Naph-1, spiro-Naph-2, or spiro-Naph-3 measured from reverse scans.

Table S4 Photovoltaic parameters of best-performing PSCs with spiro-Naph, spiro-Naph-1, spiro-Naph-2, or spiro-Naph-3 for Fig. S9.

HTM	V_{oc} (V)	J_{sc} (mA cm^{-2})	FF (%)	PCE (%)
spiro-Naph	1.15	25.12	80	23.03
spiro-Naph-1	1.16	25.01	76	22.15
spiro-Naph-2	1.13	24.79	76	21.21
spiro-Naph-3	1.13	24.86	75	21.08

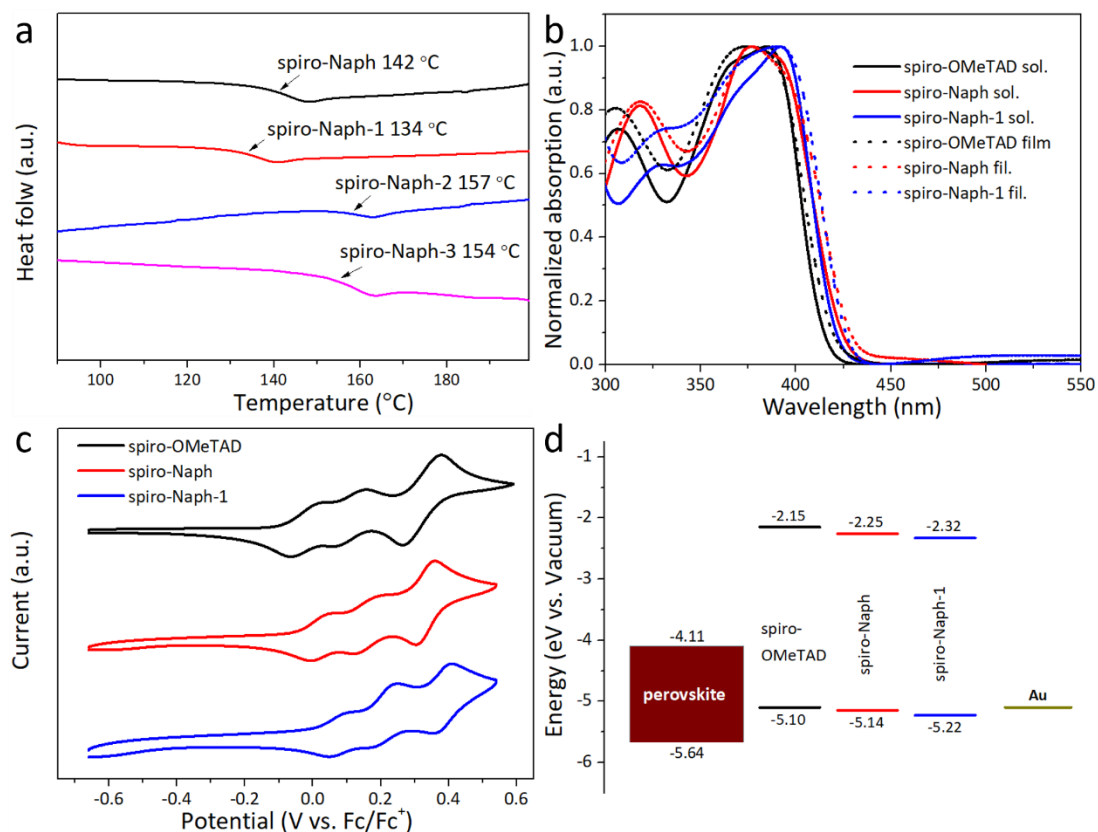


Fig. S14 (a) DSC curves, (b) UV-Vis absorption spectra in DCM solution or film state, (c) CV curves, (d) energy-level diagram of the device with studied HTMs

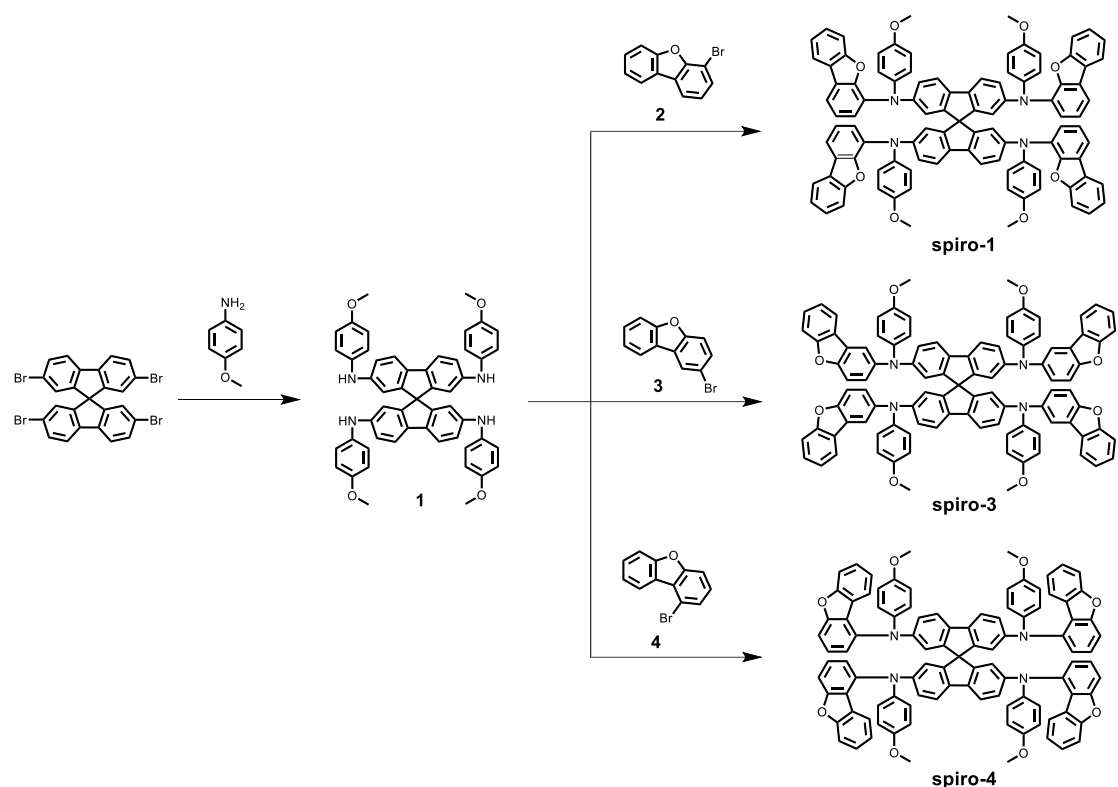
Table S5 Photophysical, electrochemical and thermal properties of spiro-OMeTAD, spiro-Naph, and spiro-Naph-1.

Molecules	λ_{\max} (nm) ^a	λ_{em} (nm) ^{a,b}	λ_{stokes} (nm) ^a	E_g (eV) ^c	HOMO (eV)	LUMO (eV) ^d	T_g (°C)
spiro-OMeTAD	386	428	42	2.95	-5.10	-2.15	122
spiro-Naph	376	472	96	2.89	-5.14	-2.25	142
spiro-Naph-1	392	455	63	2.90	-5.22	-2.32	134

^a Measured in dichloromethane solution; ^b Excited at λ_{\max} ; ^c Calculated from the onset of the absorption spectra for solid-state film.

Synthesis for spiro-2 analogues

Compound 1 and spiro-2 were mainly synthesized according to previous report with an optimized process in our lab.³⁻⁵



Scheme S1 Synthesis procedures of spiro-1, spiro-3, and spiro-4.

spiro-1

Compound 1 (0.3 mmol, 0.24 g), compound 2 (4-bromodibenzofuran, 1.8 mmol, 480 mg), tri-tert-butylphosphonium tetrafluoroborate (30 mg), and potassium and toluene (20 mL) were added to a 50 mL round-bottomed flask, degassed with nitrogen, Then, tris(dibenzylideneacetone)dipalladium(0) (30 mg) were added to the reaction mixture, then heated to reflux for 48 h with stirring, cooled to room temperature, diluted with 20 mL of dichloromethane. Then, 50 mL of water was added, followed by extracting 4 times with dichloromethane. The obtained organic phases were combined and concentrated by rotary evaporation, and the obtained crude product was purified by column chromatography (dichloromethane : petroleum ether volume ratio = 2:1) to obtain target material which was washed several times with the mixed solvent of ethyl acetate and petroleum ether (98 mg, yield 22%). ^1H NMR (500 MHz, DMSO) δ 8.09 (d, $J = 7.5$ Hz, 4H), 7.91 (d, $J = 7.7$ Hz, 4H), 7.54 – 7.23 (m, 20H), 7.02 (d, $J = 7.7$ Hz, 4H), 6.86 (m, 16H), 6.30 (m, 4H), 3.72 (s, 12H). ^{13}C NMR (100 MHz, DMSO- d_6) δ 155.97, 155.60, 150.29, 149.80, 147.02, 139.92, 134.96, 131.96, 128.11, 126.11, 125.33, 124.77, 124.41, 123.98, 123.64, 121.66, 121.21, 120.87, 117.60, 116.04, 115.05, 111.97, 65.65, 55.65. HR-MS (MALDI-TOF) m/z [M-H] calcd. For ($\text{C}_{101}\text{H}_{68}\text{N}_4\text{O}_8$): 1464.5037; found: 1464.5720.

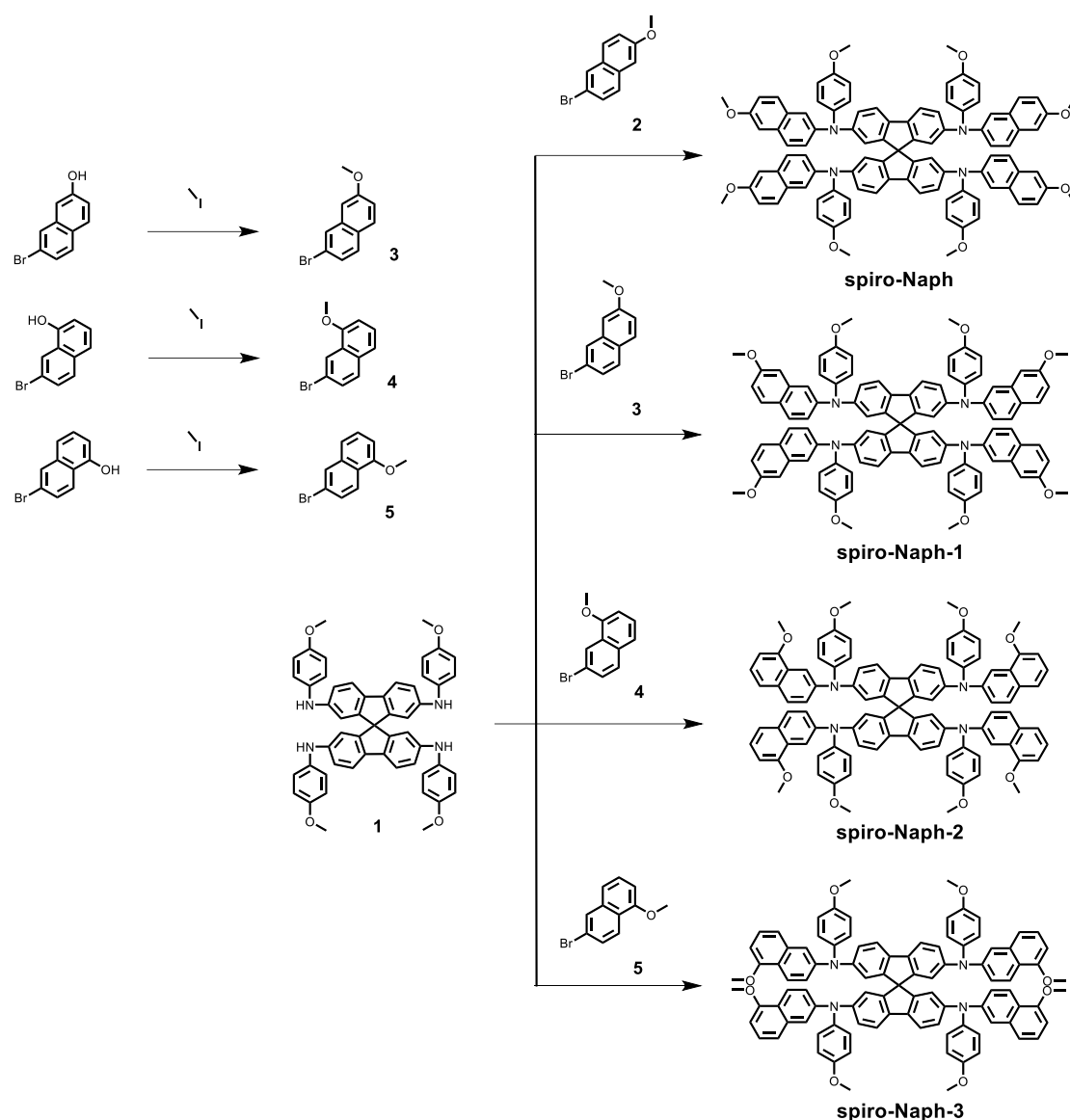
spiro-3

Compound 1 (0.3 mmol, 240 mg), compound 3 (2-bromodibenzofuran, 1.8 mmol, 480 mg), potassium tert-butoxide (0.9 g, 8 mmol), $\text{Pd}(\text{OAc})_2$ (112 mg, 0.5 mmol), $\text{P}(\text{tBu})_3$

(0.1 M in toluene, 0.5 mL) were added into a 50 mL flask and degassed using Ar. Then 30 mL dry toluene was injected in to the flask and degassed using Ar. The reaction solution was kept with stirring at reflux for 48 h. After cooling to R.T., the mixture was diluted by 30 mL CH₂Cl₂ and washed with 50 mL deionized water for 3 times. The organic phase was dried by Na₂SO₄, and removed solvent using a rotary evaporator. After drying, the solid is purified by column chromatography (dichloromethane) to obtain the product as canary yellow solid which was washed several times with the mixed solvent of ethyl acetate and petroleum ether (231 mg, yield 53%). ¹H NMR (500 MHz, DMSO-d₆) δ 7.97 (d, *J* = 7.7 Hz, 4H), 7.72 (d, *J* = 2.2 Hz, 4H), 7.65 (d, *J* = 8.3 Hz, 4H), 7.555 – 7.39 (m, 12H), 7.29 (t, *J* = 7.6 Hz, 4H), 7.04 (dd, *J* = 8.8, 2.2 Hz, 4H), 6.90 (m, 16H), 6.72 (dd, *J* = 8.3, 2.0 Hz, 4H), 6.35 (d, *J* = 2.0 Hz, 4H), 3.73 (s, 12H). ¹³C NMR (100 MHz, DMSO-d₆) δ 156.54, 155.97, 152.16, 149.88, 147.73, 143.52, 140.90, 134.55, 128.21, 126.45, 125.07, 123.78, 123.38, 121.68, 121.21, 120.78, 117.15, 115.98, 115.27, 112.83, 112.12, 65.65, 55.63. HR-MS (MALDI-TOF) *m/z* [M-H] calcd. For (C₁₀₁H₆₈N₄O₈): 1464.5037; found: 1464.5250.

spiro-4

Compound 1 (0.3 mmol, 0.24 g), compound 4 (1-bromodibenzofuran, 1.8 mmol, 480 mg), tri-tert-butylphosphonium tetrafluoroborate (30 mg), and potassium and toluene (20 mL) were added to a 50 mL round-bottomed flask, degassed with nitrogen, Then, tris(dibenzylideneacetone)dipalladium(0) (30 mg) were added to the reaction mixture, then heated to reflux for 48 h with stirring, cooled to room temperature, diluted with 20 mL of dichloromethane. Then, 50 mL of water was added, followed by extracting 4 times with dichloromethane. The obtained organic phases were combined and concentrated by rotary evaporation, and the obtained crude product was purified by column chromatography (dichloromethane : petroleum ether volume ratio = 2:1) to obtain target material which was washed several times with the mixed solvent of ethyl acetate and petroleum ether (264 mg, yield 60%). ¹H NMR (500 MHz, DMSO) δ 7.51 (m, 12H), 7.34 (d, *J* = 8.3 Hz, 4H), 7.21 (t, *J* = 7.8 Hz, 4H), 7.12 – 6.99 (m, 12H), 6.98 – 6.85 (m, 12H), 6.80 (t, *J* = 7.6 Hz, 4H), 6.64 (d, *J* = 1.9 Hz, 4H), 6.55 (dd, *J* = 8.3, 1.9 Hz, 4H), 3.74 (s, 12H). ¹³C NMR (101 MHz, DMSO-d₆) δ 157.20, 156.29, 155.47, 150.23, 146.93, 142.16, 140.68, 134.90, 128.95, 127.32, 125.77, 123.14, 122.68, 122.23, 121.39, 120.99, 120.62, 118.93, 116.44, 115.22, 111.35, 108.06, 65.45, 55.68. HR-MS (MALDI-TOF) *m/z* [M-H] calcd. For (C₁₀₁H₆₈N₄O₈): 1464.5037; found: 1464.4872.



Scheme S2 Synthesis procedures of spiro-Naph analogues.

Synthesis of spiro-Naph analogues

spiro-Naph⁶(Different synthetic route was used to synthesize it compared with the report)

Compound **1** (0.3 mmol, 240 mg), compound **2** (2-bromo-6-methoxynaphthalene, 1.8 mmol, 430 mg), potassium tert-butoxide (0.9 g, 8 mmol), Pd(OAc)₂ (112 mg, 0.5 mmol), P(tBu)₃ (0.1 M in toluene, 0.5 mL) were added into a 50 mL flask and degassed using Ar. Then 30 mL dry toluene was injected in to the flask and degassed using Ar. The reaction solution was kept with stirring at reflux for 48 h. After cooling to R.T., the mixture was diluted by 30 mL CH₂Cl₂ and washed with 50 mL deionized water for 3 times. The organic phase was dried by Na₂SO₄, and removed solvent using a rotary evaporator. After drying, the solid is purified by column chromatography (CH₂Cl₂/PE = 3:1) to obtain the product as canary yellow solid which was washed several times with the mixed solvent of ethyl acetate and petroleum ether (0.33 g). ¹H NMR (500 MHz, DMSO-d₆) δ 7.67 (d, *J* = 8.9 Hz, 4H), 7.49 (dd, *J* = 17.0, 8.6 Hz, 8H), 7.23 (d, *J* = 22.7 Hz,

8H), 7.06 (t, $J = 9.5$ Hz, 8H), 6.97 (d, $J = 8.5$ Hz, 8H), 6.88 (d, $J = 8.4$ Hz, 8H), 6.78 (d, $J = 8.3$ Hz, 4H), 6.37 (d, $J = 1.9$ Hz, 4H), 3.83 (s, 12H), 3.75 (s, 12H). Moreover, the synthesized molecule also exhibits same spectroscopic properties with the reported therein.

compound 3

Under the protection of N_2 , Cs_2CO_3 (1.5 g) and tetrahydrofuran (20 mL) were added into a 100 mL flask, the reaction mixture was kept with stirring at ice bath. Then, 2-bromo-7-hydroxynaphthalene (1 g, 4.48 mmol) dissolved in *N,N*-dimethylformamide (15 mL) were injected to the flask. After around 1 h, the methyl iodide (1.5 mL) were injected to the flask. The reaction mixture was kept with stirring at R.T. overnight. Then the mixture was poured into cold sodium sulfate aqueous solution, the white solid precipitated. The crude product was filtered to obtain compound 3 (0.95 g). 1H NMR (500 MHz, $DMSO-d_6$) δ 8.08 (d, $J = 1.8$ Hz, 1H), 7.85 (d, $J = 9.0$ Hz, 1H), 7.80 (d, $J = 8.7$ Hz, 1H), 7.46 (dd, $J = 8.7, 2.0$ Hz, 1H), 7.33 (d, $J = 2.5$ Hz, 1H), 7.20 (dd, $J = 9.0, 2.6$ Hz, 1H), 3.87 (s, 3H).

spiro-Naph-1

spiro-Naph-1 was synthesized following the same procedure to prepare spiro-Naph. Compound 3 (2-bromo-7-methoxynaphthalene, 1.8 mmol, 430 mg) was used instead of compound 2. The crude product is purified by column chromatography ($CH_2Cl_2/PE = 2:1$) to obtain the product as canary yellow solid which was washed several times with the mixed solvent of ethyl acetate and petroleum ether (0.19 g). 1H NMR (500 MHz, $DMSO-d_6$) δ 7.68 (d, $J = 9.7$ Hz, 4H), 7.62 (d, $J = 8.9$ Hz, 4H), 7.55 (d, $J = 8.3$ Hz, 4H), 7.11 (d, $J = 1.7$ Hz, 4H), 7.03 – 6.94 (m, 16H), 6.88 (m, 16H), 6.45 (d, $J = 1.9$ Hz, 4H), 3.75 (s, 12H), 3.71 (s, 12H). ^{13}C NMR (125 MHz, $DMSO-d_6$) δ 158.26, 156.59, 149.77, 146.99, 146.13, 140.20, 135.86, 135.56, 129.42, 128.80, 127.65, 124.84, 123.28, 121.19, 120.29, 117.75, 117.10, 115.44, 105.48, 65.55, 55.66, 55.43.

compound 4

compound 4 was synthesized following the same procedure to prepare compared compound 3. 7-bromo-1-hydroxynaphthalene was used instead of 2-bromo-7-hydroxynaphthalene. The crude product is purified by column chromatography ($CH_2Cl_2/PE = 2:1$) to obtain the product as white solid (0.81 g). 1H NMR (500 MHz, $DMSO$) δ 8.28 (d, $J = 1.8$ Hz, 1H), 7.86 (d, $J = 8.8$ Hz, 1H), 7.65 (dd, $J = 8.7, 2.0$ Hz, 1H), 7.54 – 7.46 (m, 2H), 7.05 (s, 1H), 3.98 (s, 3H).

spiro-Naph-2

spiro-Naph-2 was synthesized following the same procedure to prepare spiro-Naph. Compound 4 (2-bromo-7-methoxynaphthalene, 1.8 mmol, 430 mg) was used instead of compound 2. The crude product is purified by column chromatography ($CH_2Cl_2/PE = 2:1$) to obtain the product as canary yellow solid which was washed several times with the mixed solvent of ethyl acetate and petroleum ether (0.28 g). 1H NMR (500 MHz, $DMSO$) δ 7.69 (d, $J = 9.0$ Hz, 4H), 7.54 (d, $J = 8.3$ Hz, 4H), 7.49 (d, $J = 2.1$ Hz, 4H),

7.38 (d, $J = 8.3$ Hz, 4H), 7.28 (t, $J = 7.9$ Hz, 4H), 7.08 (dd, $J = 8.9, 2.3$ Hz, 4H), 6.97 (d, $J = 8.9$ Hz, 8H), 6.92 – 6.83 (m, 16H), 6.37 (d, $J = 2.0$ Hz, 4H), 3.79 (s, 12H), 3.76 (s, 12H). ^{13}C NMR (126 MHz, DMSO) δ 156.38, 154.23, 149.80, 147.18, 145.25, 140.45, 135.46, 130.46, 128.88, 127.24, 126.19, 124.94, 123.54, 123.19, 121.19, 120.21, 117.63, 115.42, 112.89, 105.35, 65.50, 55.76, 55.61.

compound 5

compound 5 was synthesized following the same procedure to prepare compared compound 3. 6-bromo-1-hydroxynaphthalene was used instead of 2-bromo-7-hydroxynaphthalene. The crude product is purified by column chromatography ($\text{CH}_2\text{Cl}_2/\text{PE} = 2:1$) to obtain the product as white solid (0.83 g). ^1H NMR (500 MHz, DMSO) δ 8.16 (d, $J = 2.0$ Hz, 1H), 8.08 (d, $J = 9.0$ Hz, 1H), 7.60 (dd, $J = 9.0, 2.0$ Hz, 1H), 7.52 – 7.44 (m, 2H), 7.02 (dd, $J = 7.1, 1.5$ Hz, 1H), 3.97 (s, 3H).

spiro-Naph-3

spiro-Naph-3 was synthesized following the same procedure to prepare spiro-Naph. Compound 5 (2-bromo-7-methoxynaphthalene, 1.8 mmol, 430 mg) was used instead of compound 2.

The crude product is purified by column chromatography ($\text{CH}_2\text{Cl}_2/\text{PE} = 2:1$) to obtain the product as canary yellow solid which was washed several times with the mixed solvent of ethyl acetate and petroleum ether (0.31 g). ^1H NMR (500 MHz, DMSO) δ 7.97 (d, $J = 9.1$ Hz, 4H), 7.52 (d, $J = 8.3$ Hz, 4H), 7.28 (t, $J = 8.0$ Hz, 4H), 7.10 (m, 8H), 7.06 – 6.97 (m, 12H), 6.92 (d, $J = 9.0$ Hz, 8H), 6.86 – 6.77 (m, 8H), 6.45 (d, $J = 2.0$ Hz, 4H), 3.94 (s, 12H), 3.76 (s, 12H). ^{13}C NMR (126 MHz, DMSO) δ 156.58, 155.32, 149.67, 146.81, 146.14, 140.08, 135.62, 127.57, 127.33, 123.51, 122.83, 121.59, 121.14, 121.07, 120.84, 119.25, 117.75, 117.38, 115.39, 103.24, 65.33, 55.72, 55.58.

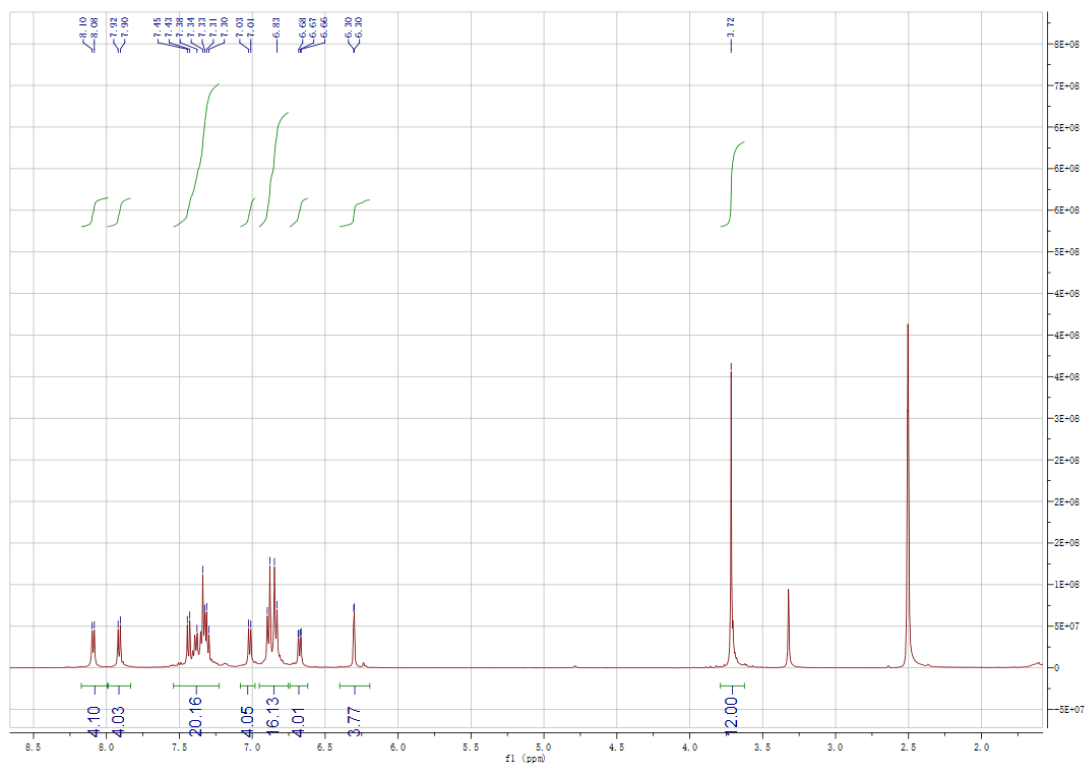


Fig. S15 ^1H NMR of spiro-1.

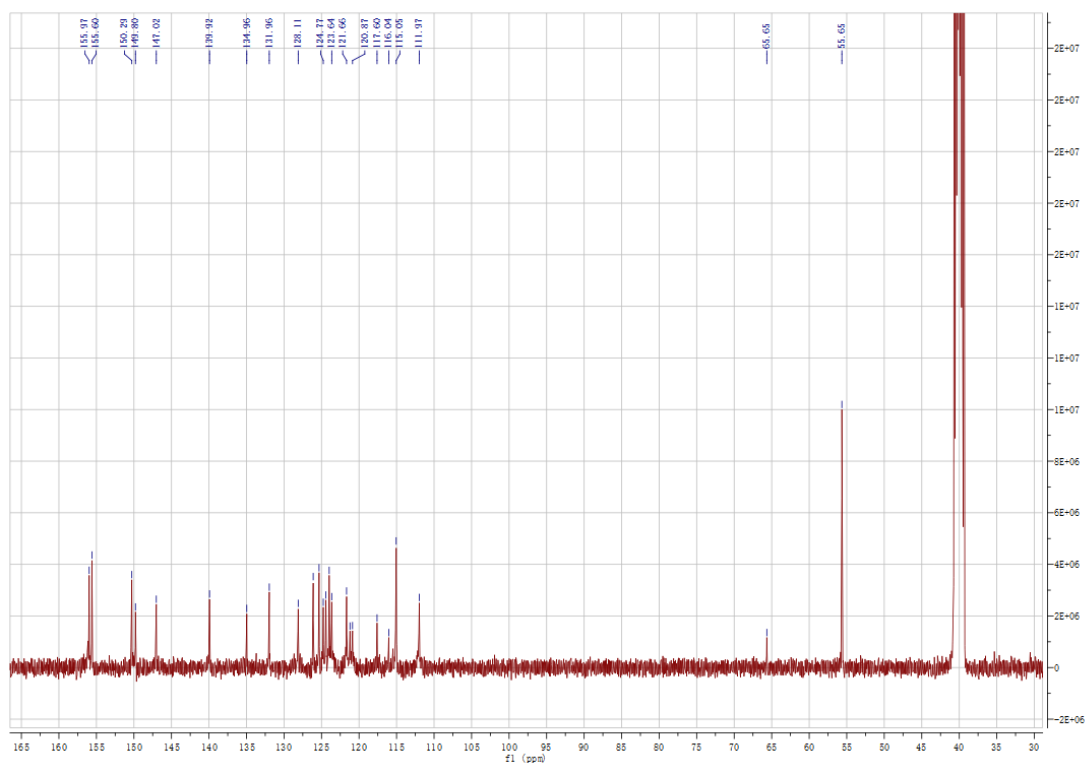


Fig. S16 ^{13}C NMR of spiro-1.

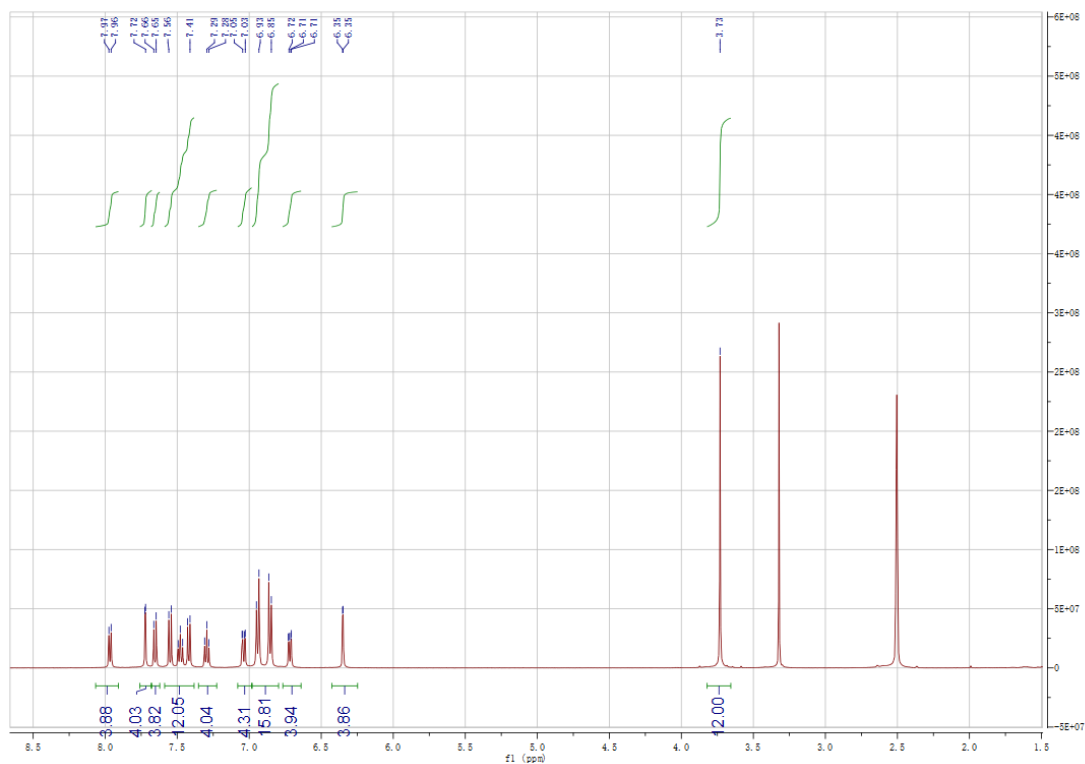


Fig. S17 ^1H NMR of spiro-3.

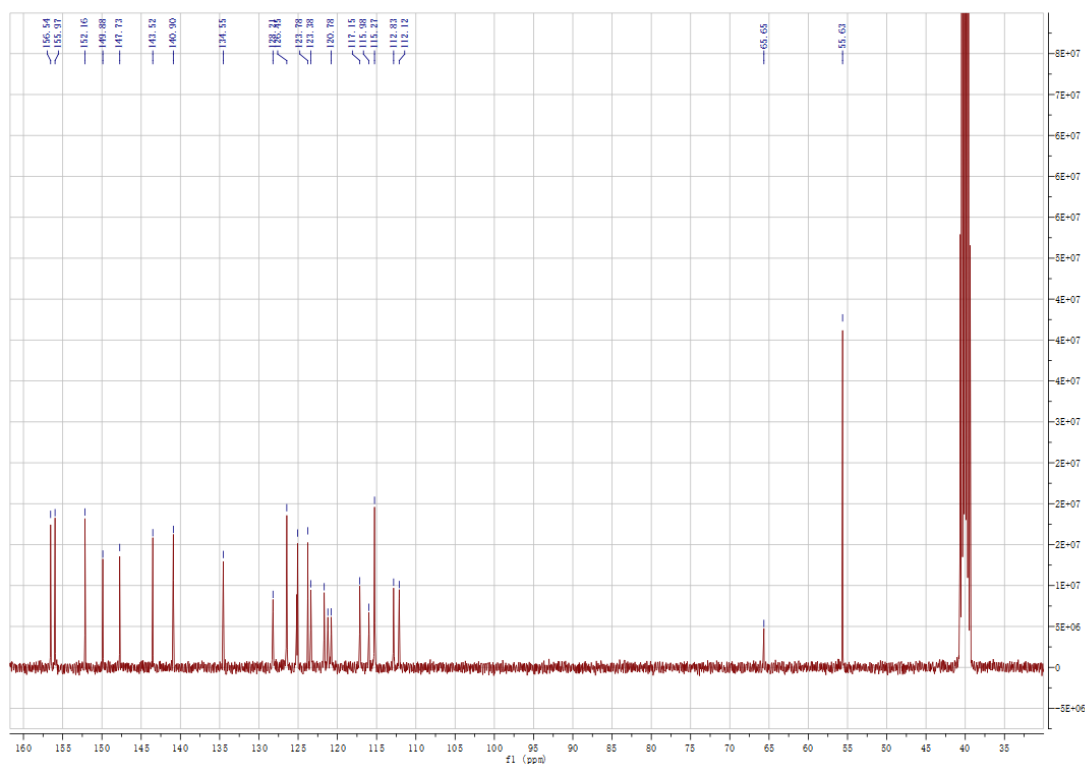


Fig. S18 ^{13}C NMR of spiro-3.

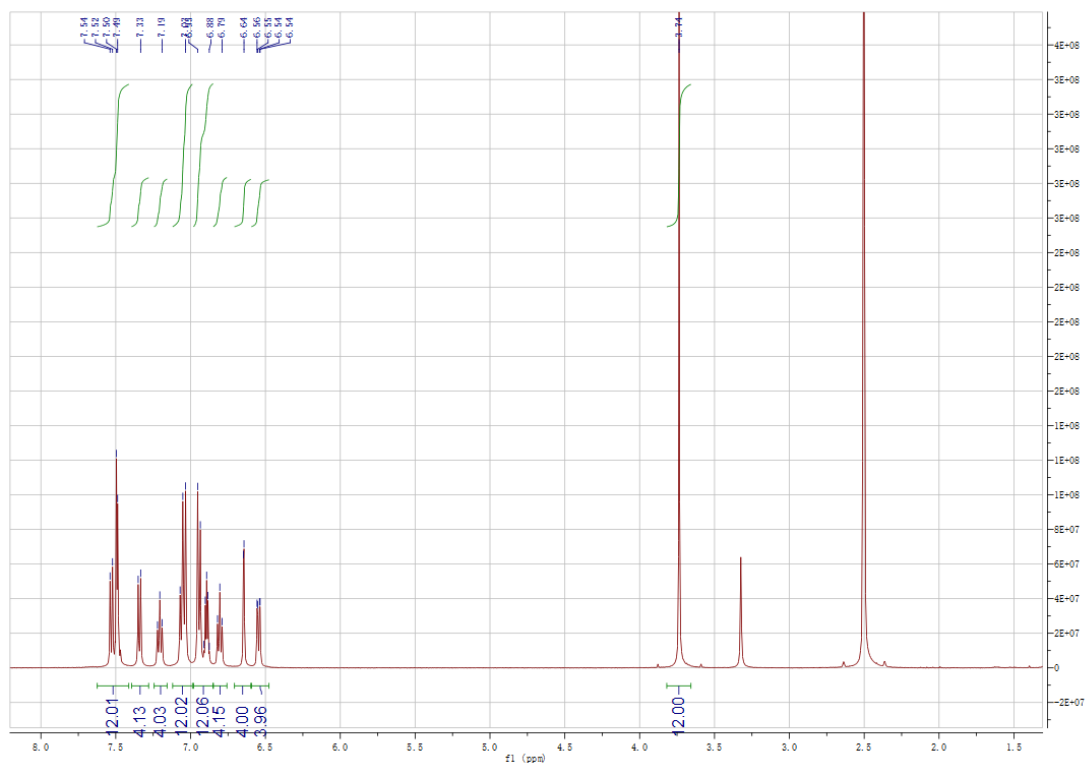


Fig. S19 ^1H NMR of spiro-4.

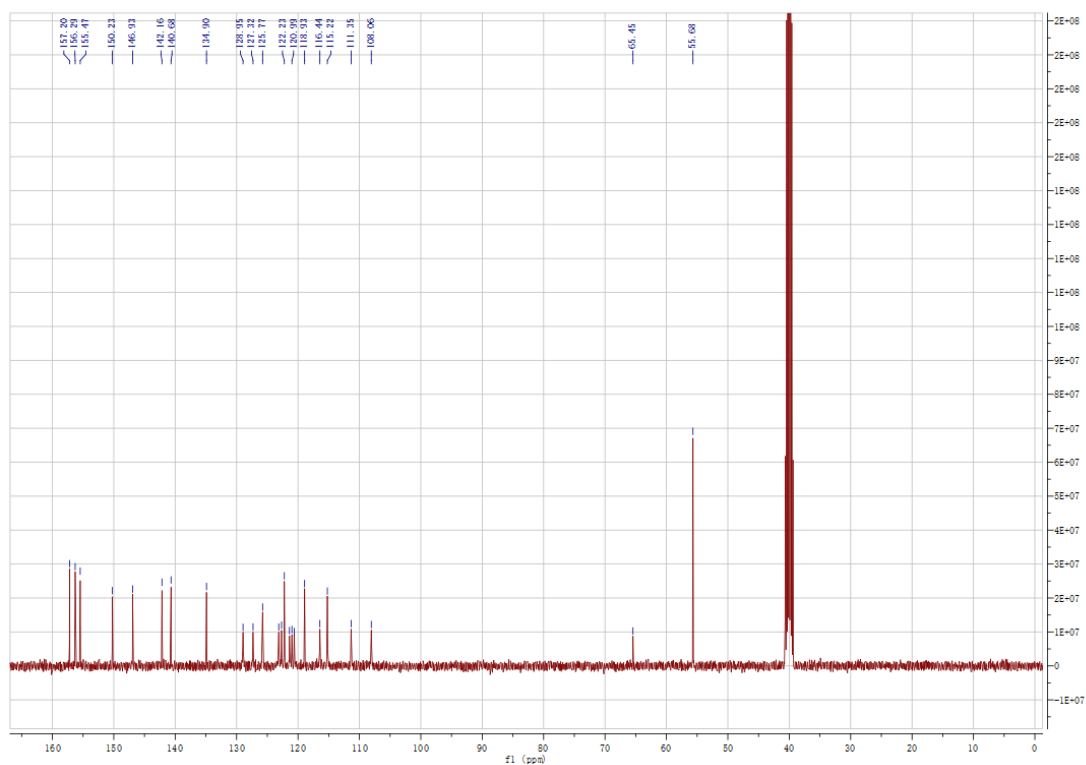


Fig. S20 ^{13}C NMR of spiro-4.

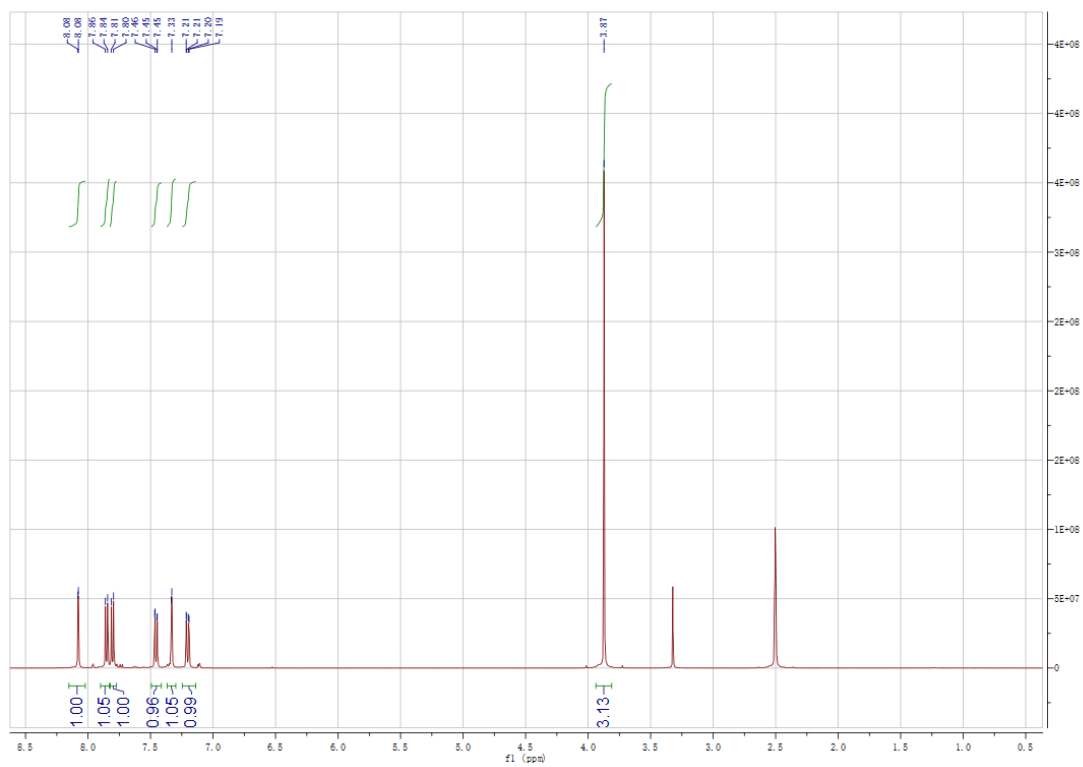


Fig. S21 ^1H NMR of compound 3.

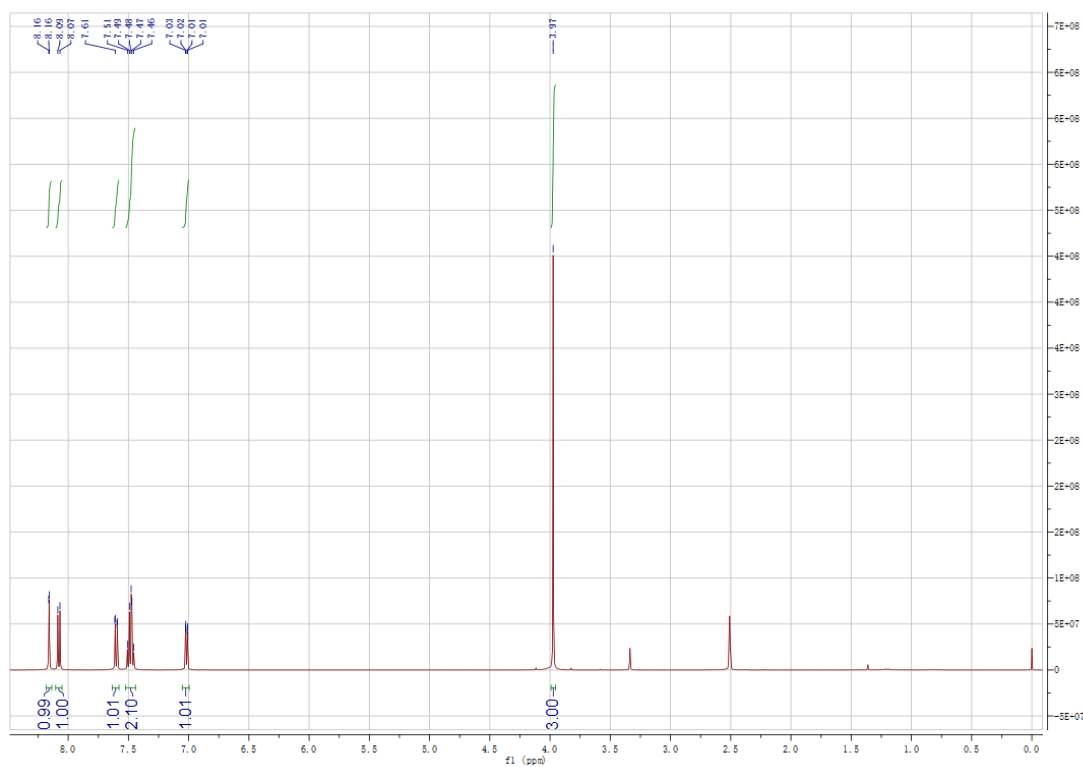


Fig. S22 ^1H NMR of compound 4.

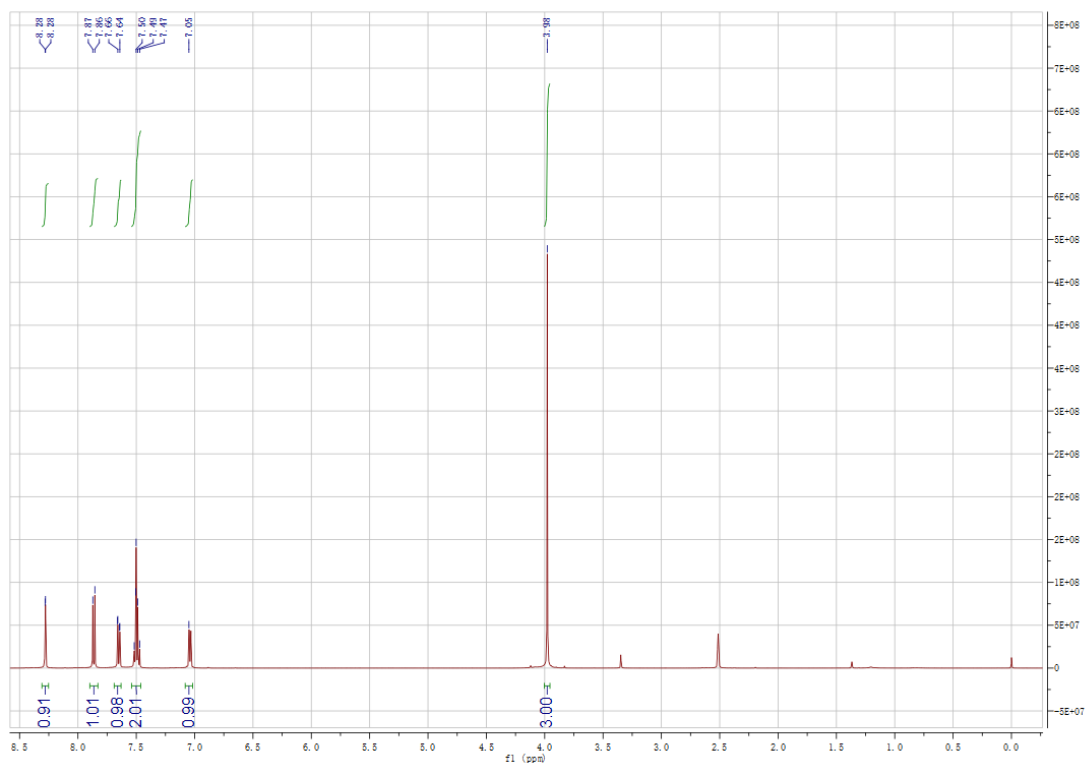


Fig. S23 ^1H NMR of compound 5.

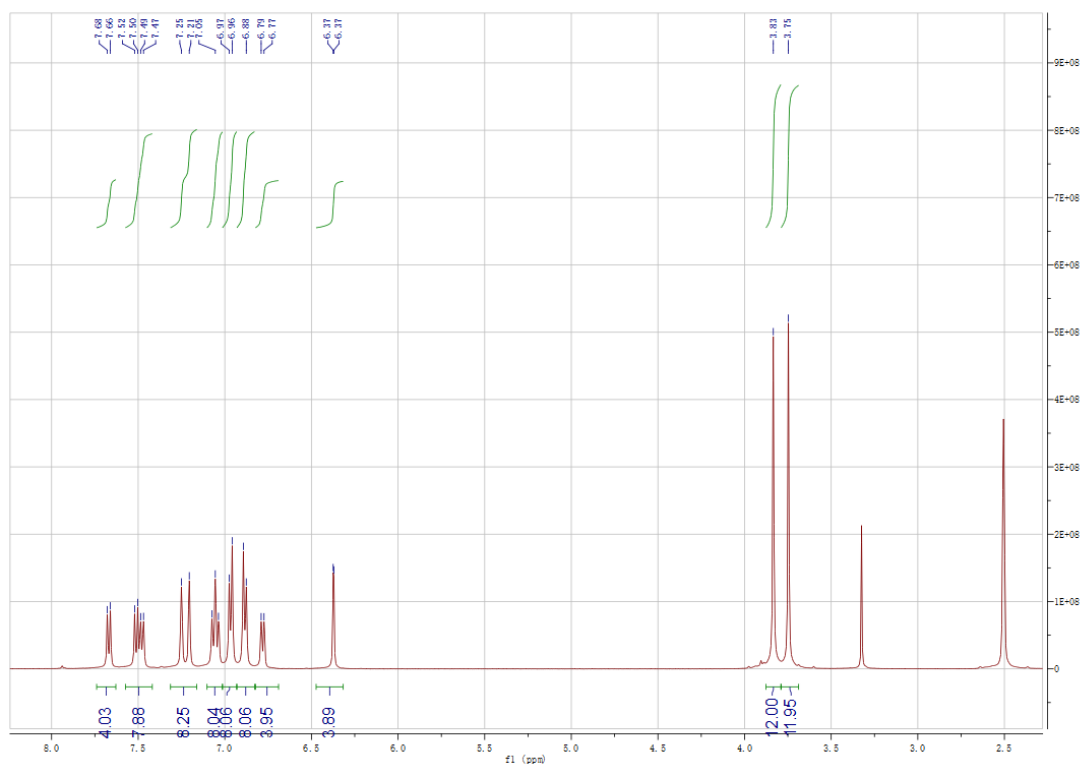


Fig. S24 ^1H NMR of spiro-Naph.

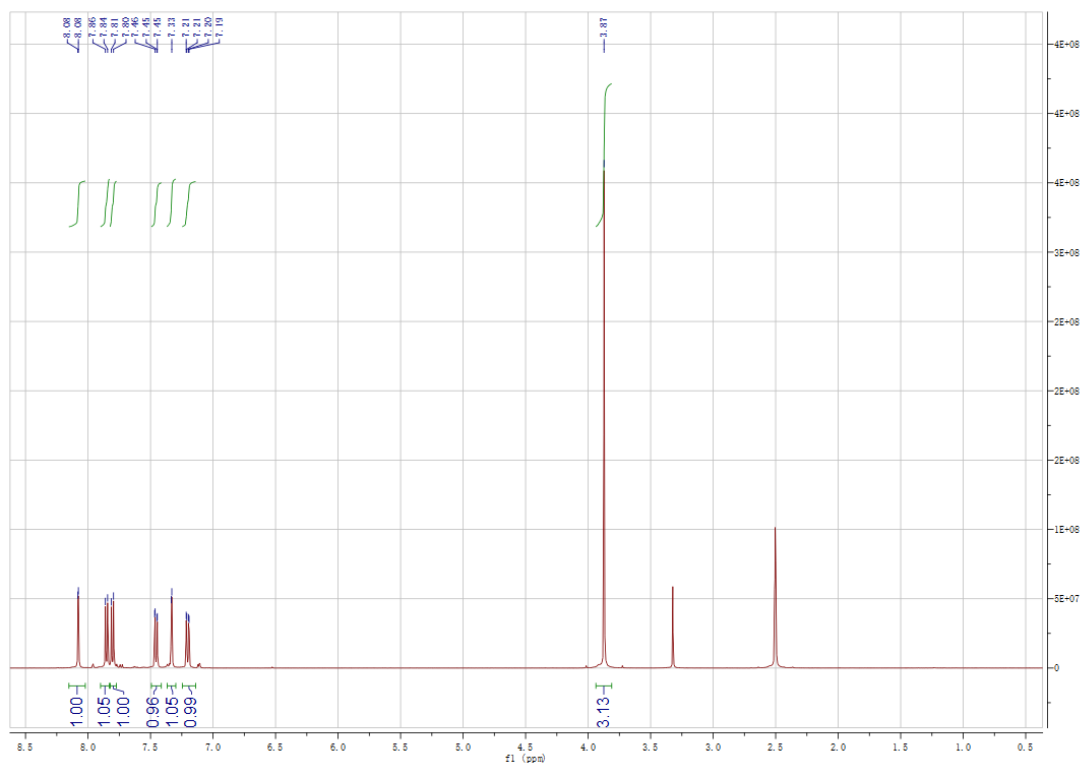


Fig. S25 ^1H NMR of compound 3.

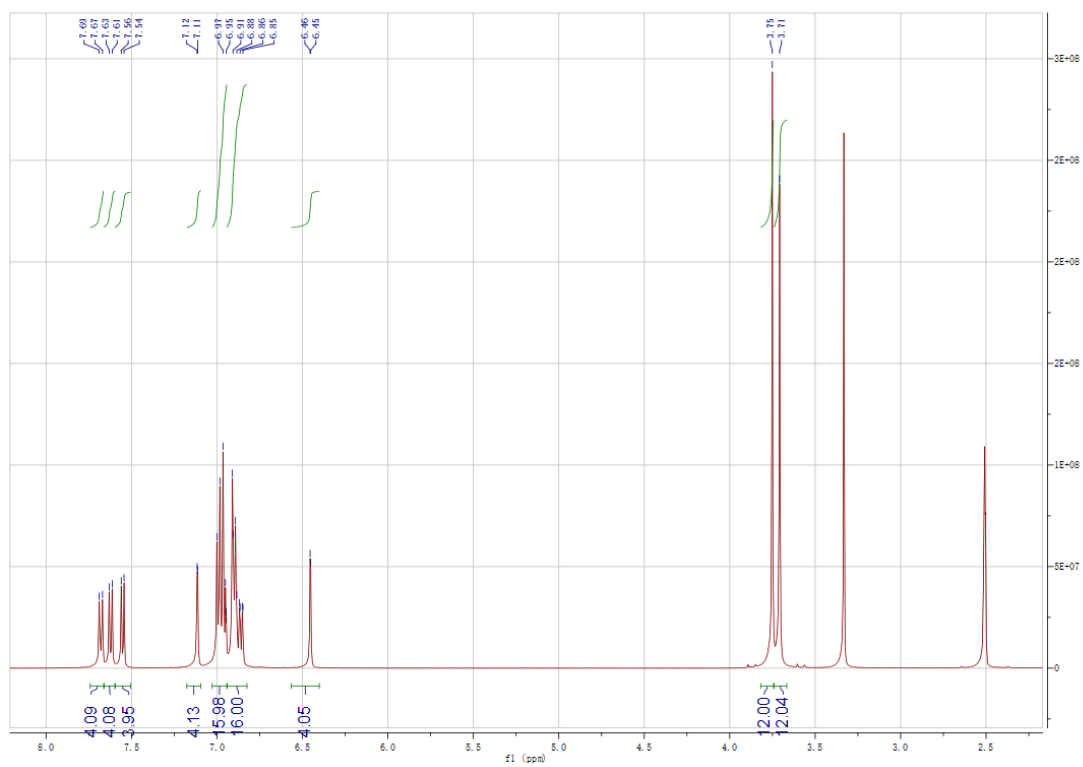


Fig. S26 ^1H NMR of spiro-Naph-1.

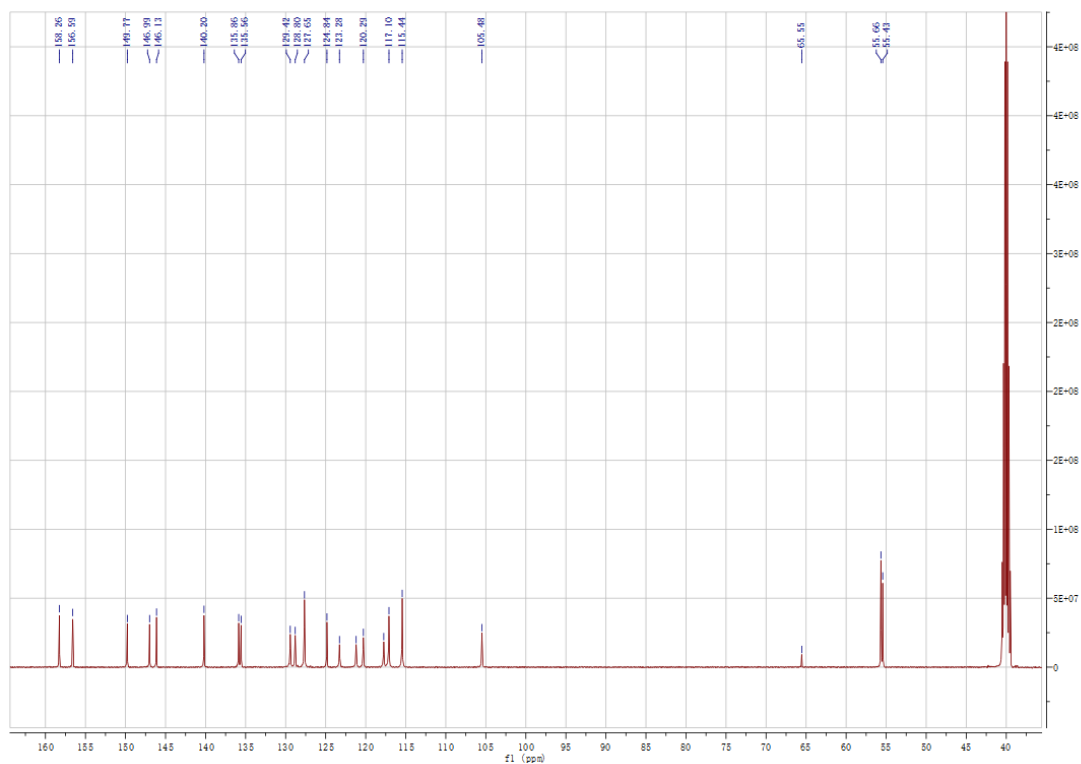


Fig. S27 ^{13}C NMR of spiro-Naph-1.

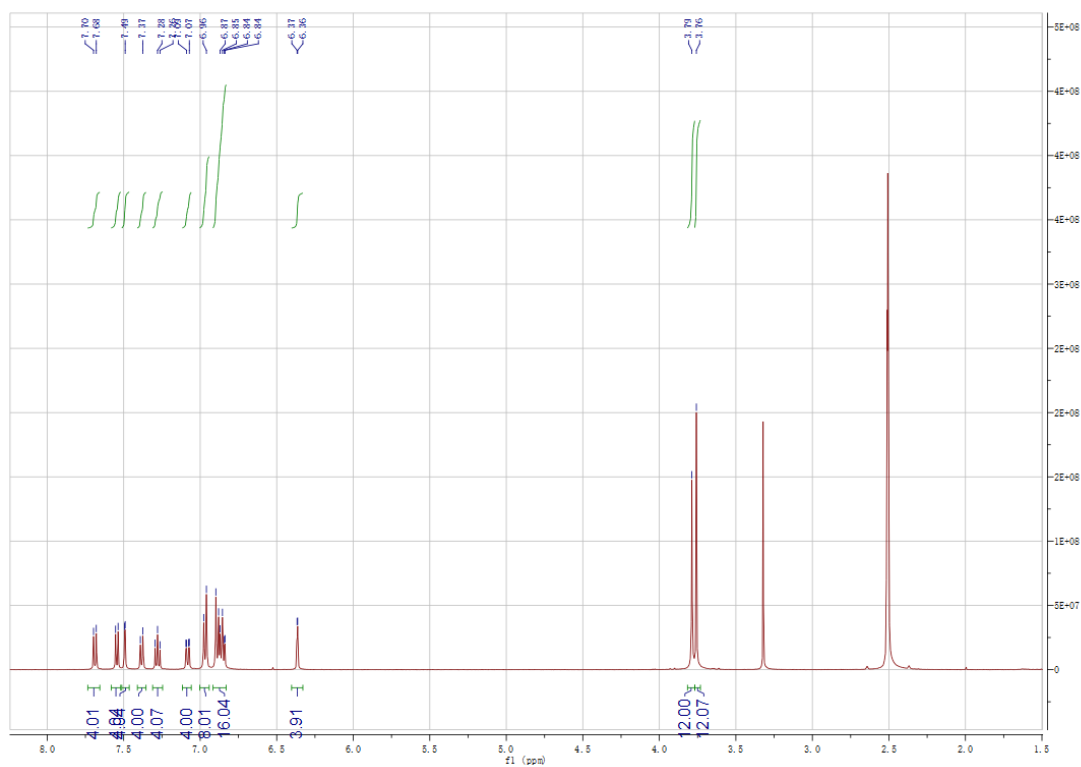


Fig. S28 ^1H NMR of spiro-Naph-2.

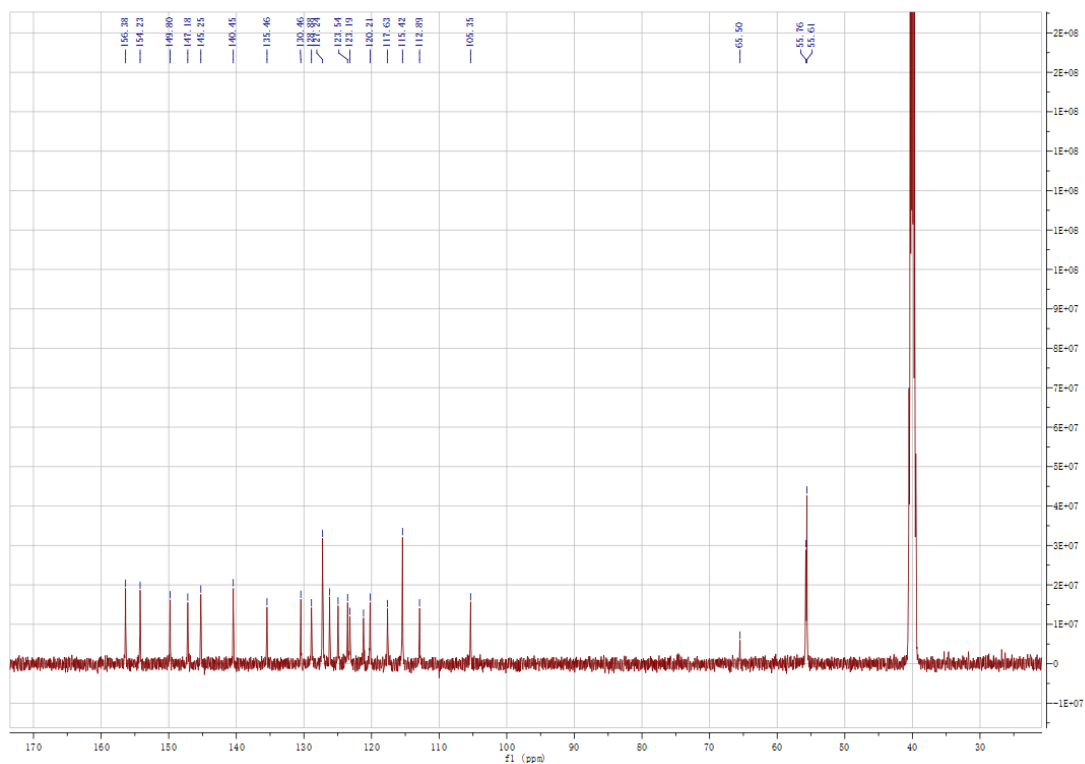


Fig. S29 ^{13}C NMR of spiro-Naph-2.

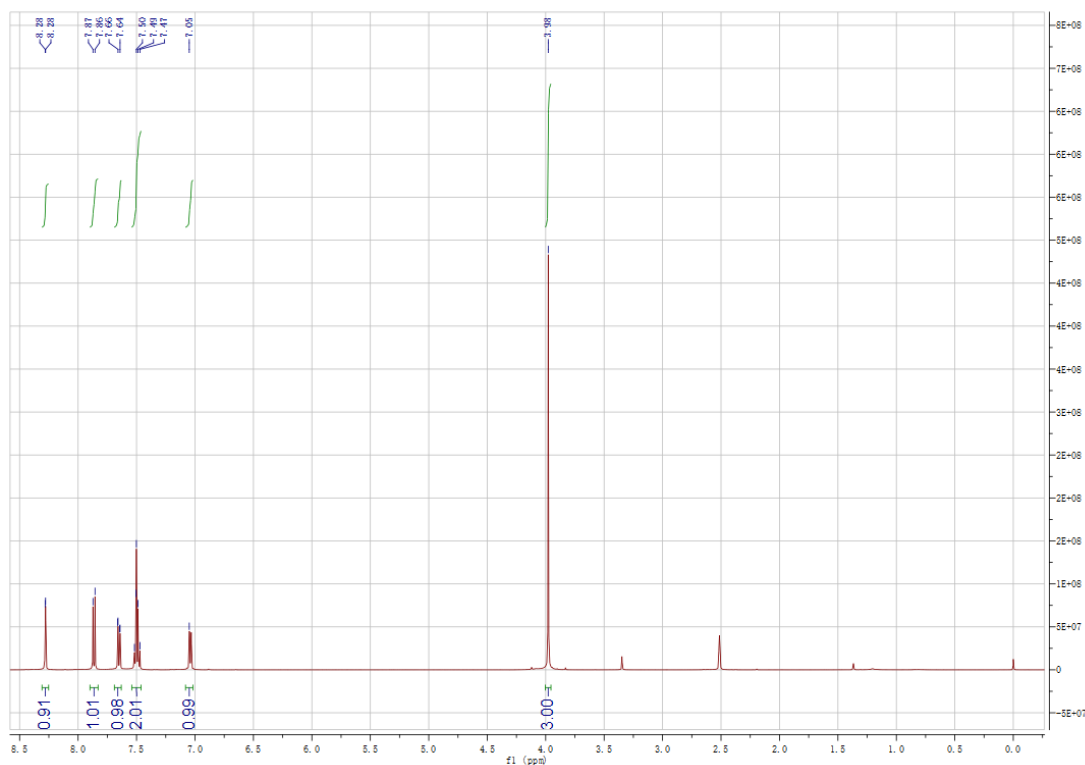


Fig. S30 ^1H NMR of compound 5.

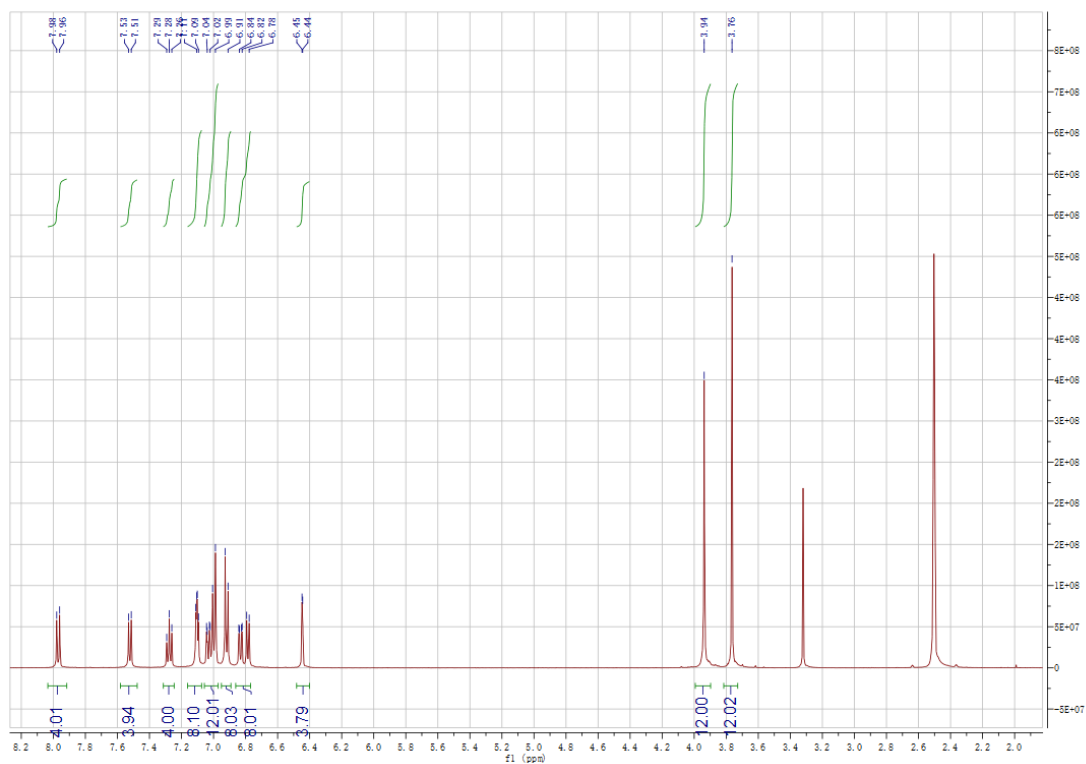


Fig. S31 ^1H NMR of spiro-Naph-3.

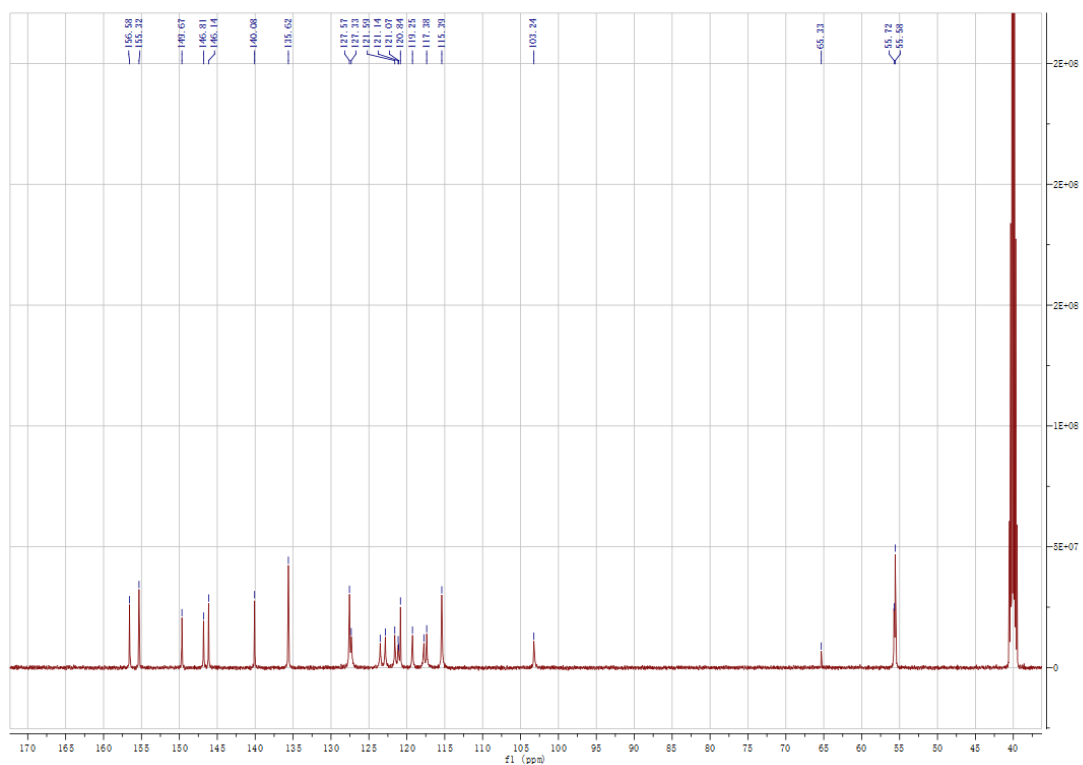


Fig. S32 ^{13}C NMR of spiro-Naph-3.

Reference

1. Y. Zhou, X. F. Zhang, M. Y. Han, N. Wu, J. L. Chen, G. Rahim, Y. H. Wu, S. Y. Dai and X. P. Liu, *Sol. Energy Mater. Sol. Cells*, 2023, **257**, 112375.
2. M. Y. Han, Y. P. Liang, J. L. Chen, X. F. Zhang, R. Ghadari, X. P. Liu, N. Wu, Y. Wang, Y. Zhou, Y. Ding, M. L. Cai, H. B. Chen and S. Y. Dai, *ChemSusChem*, 2022, **15**, e202201485.
3. N. J. Jeon, H. Na, E. H. Jung, T.-Y. Yang, Y. G. Lee, G. Kim, H.-W. Shin, S. Il Seok, J. Lee and J. Seo, *Nature Energy*, 2018, **3**, 682-689.
4. X. Zhang, X. Liu, N. Wu, R. Ghadari, M. Han, Y. Wang, Y. Ding, M. Cai, Z. Qu and S. Dai, *J. Energy Chem.*, 2022, **67**, 19-26.
5. Y. P. Liang, J. L. Chen, X. F. Zhang, M. Y. Han, R. Ghadari, N. Wu, Y. Wang, Y. Zhou, X. P. Liu and S. Y. Dai, *J. Mater. Chem. C*, 2022, **10**, 10988-10994.
6. M. Jeong, I. W. Choi, K. Yim, S. Jeong, M. Kim, S. J. Choi, Y. Cho, J.-H. An, H.-B. Kim, Y. Jo, S.-H. Kang, J.-H. Bae, C.-W. Lee, D. S. Kim and C. Yang, *Nature Photonics*, 2022, **16**, 119-125.